Characteristics of Air Impingement from an Orifice on a Target Plate

Dr.Adnan A. Abdul Rasool
Engineering College, University of Al-Mustansiriyah /Baghdad
Email: adn1954@yahoo.com

Received on: 22/12/2011 & Accepted on: 8/11/2012

ABSTRACT

The present work is an experimental and numerical CFD study of air impingement from orifices of different sizes in the range of (10-40) mm with a step increase of 10 mm. The impinging jet strikes the target plate at the stagnation point, converted to a wall jet beyond the stagnation zone in the outward radial direction on the target plate. Measurements of pressure coefficient (Cp) at points in plate centre and other points in the radial direction from stagnation point on the target plate show that pressure coefficients reduces gradually in the outward direction reflecting the same behavior of velocity distribution of the impinging jet ..The calculated average values of the pressure coefficients Cpavg on the total target plate area are reduced as the target plate – orifice distance is increased and its values are in the range of 0.3-0.7 with the higher jet velocity having the greater value of Cpavg for the tested axial distances in the range of 50-120 mm. Average pressure coefficient for different axial distances are calculated and are in the range of 0.4-0.6 with the higher values are noticed to be for the smaller tested orifice sizes reflecting a concentration of pressures for the small sizes of the orifice. This concentration of pressure of small orifices is attributed to the flow condition of the small orifice relative to the big orifice size where the presence of cross flow within the stagnation region of big orifice sizes tends to reduce static pressures and reduce peak heat transfer coefficients, this cross flow is confirmed by the velocity analysis using CFD numerical analysis zone at the stagnation zone. The percentages of the wall jet relative to the impinging jet velocities are discussed, where smaller orifice sizes are shown to have greater velocity percentages especially at the higher tested jet velocities.

Keywords: Jet impingement; Pressure coefficient; Turbulence; *k*– ε model.

خصائص نفث الهواء من ثقب على صفيحة

الخلاصة

يهدف البحث لإجراء دراسة عملية وعددية لنفث الهواء من ثقوب بأحجام متغيرة ضمن المدى (١٠-٤٠ ملم). يرتطم الهواء بصفيحة في منطقة الركود ويتحول إلى جريان أفقي قرب الصفيحة. أظهرت النتائج ان قيم معامل الضغط (Cp) تقل تدريجياً بالإتجاه الأفقي بعيداً عن منطقة الركود عاكسةً نفس تصرف توزيع السرعة في منطقة النفث من الثقب. القيم المستحصلة من حسابات قيم (Cp_{av}) المتوسطة على مساحة الصفيحة كانت ضمن الحدود (٠,٣-٠,٧) حيث كانت القيم الكبيرة

https://doi.org/10.30684/etj.31.7A8
2412-0758/University of Technology-Iraq, Baghdad, Iraq

للسرع العالية التي تم اختبارها وفي مدى المسافات من الثقب إلى الصفيحة والتي هي بحدود (٥٠-١٢٠ ملم) القيم المتوسطة لـ(Cp_{av}) ولمسافات متغيرة، تم حسابها ووجد أنها ضمن المدى (٠,٤-٠,٦) حيث كانت القيم العالية للثقوب الصغيرة حيث يكون تركيز النفث أكبر منه مما هو في حالة الثقوب الكبيرة وبيّن الحل العددي لتوزيع السرع عدم وجود سرع أفقية في حالة الثقوب الصغيرة مقارنة بالثقوب الكبيرة مما يعمل على إنقاص قيم معاملات إنتقال الحرارة في منطقة الركود. تم قياس نسب السرع في المنطقة القريبة من سطح الصفيحة حيث أظهرت الثقوب الصغيرة نسب أعلى منها في حالة أحجام الثقوب الكبيرة خصوصاً في حالة السرع العالية.

NOMENCLATURE

A	Plate surface area	
C_1 , C_2 , $C\mu$, Ec	Coefficients in dissipation Rate	
$Cp = P / 1/2 \rho Uj^2$	Pressure coefficient	
$Cp_{av} = \int CpdA / \int dA$	Average Pressure coefficient	
d	Orifice Diameter	(mm)
k	Coefficient, constant	
K	Turbulent Kinetic Energy	(m^2/sec^2)
P	Static Pressure	(N/m^2)
r	Radial Distance	(mm)
Uj	Jet Velocity	(m/sec)
Xo	Axial Distance from orifice	(mm)

INTRODUCTION

Air impingement is widely used in different industrial applications as electronics cooling, glass manufacturing industry, gas turbines blade internal cooling, etc. This technique is preferred due to high rate of heat removal especially at the stagnation zone of the impingement. Beyond this zone the jet is converted to a wall jet where the heat removal reduces asymptotically with a high rate. The heat transfer zones and characteristics and mechanism of heat removal are studied by different author's researches. Jung-Yang et .al [1] carried out an experimental study of air impingement orthogonally on a flat plate , the air jet is constrained to exit in two opposite directions . Four orifice diameters of 3, 4 6 and 9 mm are used, jet Reynolds number is in the range of 30,000 – 67,000 and the orifice to plate distance is fixed to (H/d) = 2.0. Their results shows that for the same Reynolds number small orifice diameter gives higher local Nusselt number, their local surface temperature measurements show that transition from impingement region to a wall jet region take place at the value of plate radius to orifice diameter ratio (r / d) near 1.0. M.Behina et.al [2] used an elliptic relaxation turbulence model (v^2–f model) to simulate the flow and heat transfer in a circular confined and unconfined impinging jet configurations .Their results show that the effect of confinement is only significant in very low orifice to plate distances (H/d<0.25) and that the flow characteristics in the orifice strongly affect the heat transfer rates , specially in the stagnation region with 30 % difference in Nu number is obtained with different velocity profiles were used.

R.J.Goldstien and A.J. Bahbahani,[.3] reported the measurement for local heat transfer to an impinging air jet with and without a cross flow of air , results show that cross flow diminishes the peak heat transfer coefficients at the large jet to plate spacing while at small spacing cross flow increase the peak heat transfer coefficients .Orifice diameter tested was 12 mm. D.Lee ,et.al [.4]examine the heat transfer from a flat plate to a fully developed ax symmetric impinging jet from a nozzle of 11 mm .Variable nozzle to plate distance ratios are tested, a maximum in heat transfer rate is noticed at the hydrodynamic transition from laminar to turbulent flow point. A.K Mohanty and A.A.Tawfek [5] studied the local heat transfer distribution on a flat plate for three nozzle diameters of 3, 5,and 7 mm for variable (H/d) values. Their results show that the heat transfer is a maximum at the impingement point and then decays exponentially with radial distance r, results are presented as a non dimensional heat transfer rate function of effective area for the nozzle. D.Lytle [.6] measured local heat transfer coefficients and static pressure distribution at low nozzle to plate spacing. Pressures are noticed to decrease monotonically with radius on target plate, it reduces to negative values at outward positions for high jet velocities, nozzle diameters tested is 6.9 and 10.9 mm .Nusselt numbers variation on the target plate is found to vary with type of flow encountered at impinging point and the location of transition point and turbulence levels in the flow. J .Mi .et al [7] performed an experimental study on the mixing performance for a nozzle, a long tube and a sharp edge orifice. The orifice is found to provide the greatest rate of mixing, with the turbulence intensity is low at orifice centre and higher at orifice edges.

Previous works shows that a significant relation exists between hydrodynamic behavior and heat dissipation rate at the stagnation point and the zone beyond it in outward direction on the target plate. E. Baydar and Y. Ozmen , [8] carried out experimental and numerical study for very high Reynolds number impingement of air on a target plate(Re = 30000-50000) with low values of non dimensional nozzle to plate spacing .There results show that a sub atmospheric region occurs on the impingement plate at nozzle to plate spacing up to 2 for Reynolds numbers studied . The numerical results obtained using the K–ε turbulence model are in agreement with experimental results except for nozzle to plate spacing less than one.

The author of present work notice that almost the heat transfer using impingement technique uses small orifice sizes in the range of (3-12 mm), and studies on relatively big orifice sizes than the mentioned range are rare .This notification imply that characteristics of orifices of such sizes are still unknown. The present work is a a study air impingement characteristics from different orifice sizes of 10, 20, 30, and 40 mm .The characteristics discussed includes jet velocity profile, static pressure distribution, kinetic energy and hydrodynamic boundary layer formed on the target plate at the wall jet region in addition to heat transfer coefficients on the plate. The flow field between the orifice zone and the target plate is analyzed numerically using finite volume CFD including the entrainment effect near orifice exit.

EXPERIMENTAL TEST RIG

The experimental test rig consist of a centrifugal blower 1.1 Kw power with a 4 inch pipe diameter with a straighter fitted at its entrance to ensure uniform flow through the pipe with low level of turbulence . The pipe length is 1.5 m , pipe length is designed to give a fully developed flow conditions at the orifice end of the pipe(assuming that fully developed conditions is attained at 10 pipe diameter length in case of turbulent flow) .Orifice is designed to fit into a covering cap sustaining the orifice plate in each set of experiments of each orifice . Jet velocity at orifice exit is fixed using a gate valve at blower inlet. Jet velocity profile is measured using a total tube 1.0 millimeter in diameter fixed on a three dimensional traversing mechanism designed for this purpose so that velocity can be measured at different axial positions away from the used orifice .

The target plate is made of Plexiglas plate 400 x 400 x 4 mm in size. The plate is designed to be hold from its two vertical edges, so as the jet exits from the orifice impinges the plate centrally. The target plate is drilled at its centre and in radial direction with holes 1.5 mm in diameter. 12 holes are used with a pitch of 6 mm , these holes are fitted with same outer diameter tubes 30 mm in length used for measuring static pressure distribution on the target plate ,starting from plate centre an away from it in the outward radial direction . Another traversing mechanism is used to measure the velocity distribution within the hydrodynamic boundary layer formed in the wall jet region which generates due to the change of flow direction of the jet from the orthogonal direction to the radial direction parallel to the plate surface. The traversing mechanism allow the velocity measurement in the upward direction at each radial position on the plate .The static holes number and locations for wall jet measurement points are pre designed to give enough data required .

A sensitive, variable inclination calibrated manometer is used for measuring the velocity dynamic head within the impinging jet and the wall jet region. The orifice to plate axial position Xo is varied by changing the distance at which the target plate is fixed relative to the orifice plate. The positions is changed so as the values of Xo will be 5,20,50,70,100,120 mm. The velocity distribution within the impinging jet is measured at the same mentioned axial positions from the orifice. Total tube is traversed at each position in radial direction to get the velocity distribution. Jet velocity examined is in the range of 7-28 m/ sec. The lay out of the experimental rig and its details are shown in Figure (1) .

NUMERICAL ANALYSIS

The flow of the impinging air from the orifice to the flat plate is analyzed using 2D finite volume K –ε code using Cartesian grid shown in Figure (2) assuming an ax symmetric plane flow and laminar or turbulent flow with quadratic interpolation scheme(Quick). A 15 x 15 non uniform mesh is used with x- direction grid lines expanding from both left right boundaries to a specified position Xo, and the y – direction grid lines expanding from the edge to the top and bottom boundaries. .A power function is used for clustering the grid mesh in both x and y directions. Boundary conditions are specified on 5 boundaries: at inlet a uniform u- velocity and V=0, at the axis of symmetry əu /əy = 0 .Wall functions are used at the impingement wall ,at the entrainment and outflow boundaries ,a constant pressure condition and the gradient of tangential velocity is set to zero. The output data contains the values of u and v velocities, static pressure (p), kinetic energy (K),

dissipation rate (ε) ,temperature and the residual source values(each iteration calculated remainder error).

The transport equations for continuity, momentum, energy, and the turbulence scales K and ε, which all have the general form.

$$\frac{\partial}{\partial x}(\rho u\phi)+\frac{\partial}{\partial y}(\rho v\phi)+\frac{\partial}{\partial z}(\rho w\phi)=\frac{\partial}{\partial x}(\Gamma\phi\frac{\partial\phi}{\partial x})$$
$$+\frac{\partial}{\partial y}(\Gamma\phi\frac{\partial\phi}{\partial y})+\frac{\partial}{\partial z}(\Gamma\phi\frac{\partial\phi}{\partial z})+S\phi \qquad \text{…..(1)}$$

Where ϕ is the dependent variable and $S\phi$ is the source term. The convection and diffusion terms for all the transport equations are identical with $\Gamma\phi$ which represent the diffusion coefficient for scalar variables and the effective viscosity μ_{eff} for vector variables. For solving the partial differential equations (1) for each variable, the control volume is divided into a number of control volumes; each volume is associated with particular dependent variable at a certain grid points. The hybrid differencing scheme is used for obtaining the discrimination equation for the three-dimensional based on the general differential equation (1). The simple algorithm by patankar (u) was applied to find the correction velocity u', v', w' and the pressure correction p' for each iteration. The dissipation term ε in the turbulence energy equation is calculated from the following equations:

$$\varepsilon=\frac{C\mu^{1/4}K^{1/2}x^{+}}{xp} \qquad \text{…..(2)}$$

if the viscous sub layer ($x^+ < 11.63$)

$$\varepsilon=\frac{C\mu^{1/4}K^{1/2}\ell n(Ec\ x^{+})}{K\ xp} \qquad \text{…..(3)}$$

if turbulent region ($x^+ > 11.63$)

In the wall flow a fixed value for ε based on the equilibrium relation. The equation for ε at the near wall is.

$$\varepsilon=\frac{C\mu^{1/2}K^{1/2}}{K\ xp} \qquad \text{…..(4)}$$

K –ε energy dissipation method is used with constants Cμ =0.09, C1=1.44, C2= 1.92, *K* = 0.4187, Ec= 9.793. Entrainment effect is used near the orifice entrance region with its maximum effect near orifice zone and entrainment velocities diminish in the forward axial positions.

RESULTS

The following is a description of the experimental and numerical results for the behavior of the jet which exits from different orifice sizes and its impingement on the target plate. The velocity distribution at axial positions of Xo= 5, 50,100 mm are shown in fig -3 as example for the orifice sizes of 10,20,30,40 mm. Example of the results for low and relatively higher jet velocities tested of 7 and 28 m / sec are shown. The figure reveals that for small orifice sizes the jet exits from the orifice with potential flow characteristics and as axial distance increases the velocity distribution tends to a bell shaped profile with a high rate of jet velocity reduction in the axial direction at which the jet transfers to a free jet with the wider formed jet covers bigger areas in the mentioned positions. As the orifice diameter increases potential flow remains for longer axial distances and then tends to a free jet at longer axial distances than smaller orifice diameters, this behavior agrees with experimental results of reference(8) .

Figure (4) shows the experimental static pressure distribution represented by the pressure coefficient Cp for orifice sizes of 10,20,30,40 mm and jet velocities of 7 and 18 m/ sec. The pressure coefficient distribution on the target plate at different axial positions given in the figure reflects the velocity distribution at these axial positions. The small orifice size covers a smaller percentage of the radial distance cover aged by the jet on the target plate. The negative or under atmospheric pressures are noticed at the outward points in the radial direction away from the stagnation at the centre of the target plate, the higher the velocity the greater the tendency to negative pressures at these points .The bigger the orifice size the bigger is the radial area cover aged by positive pressures on the target plate. The higher the jet velocity is with greater pressure coefficients on the plate. Figure (5) declares the average pressure coefficients on the target plate Cpavg ,as the axial distance increases the coefficient decreases gradually with its maximum value at the potential jet flow region and the higher jet velocities tend to give higher pressure coefficients on the plate .The average pressure coefficients on the target plate area reduces as the distance from the target plate increases .Its values are in the range of 0.7 at Xo = 5 mm and tends to the value of 0.3 as Xo increases to 120 mm . Figure (6) reveals the behavior of average pressure coefficient at different axial locations with orifice diameter , the smaller the orifice diameter gives relatively higher average pressure coefficients, with the average pressure coefficients calculated on the target plate area are in the range of about 0.6 to 0.4 and the higher jet velocities give higher coefficients values. This behavior indicates the higher concentration of the jet on the target plate in case of smaller orifice size relative to the big orifice size even though bigger orifice sizes give higher potential velocities at the nearer distances to the target plate as declared by the velocity distributions discussed earlier in Figure (3). This behavior can be discussed on the basis of energy dissipation within the jet flow through its exit from the orifice till the impingement on the target plate.

Figure (7)and Figure (8) show the CFD numerical results for the velocity distribution represented by velocity arrays and static pressure distribution (P),turbulent kinetic energy of the jet (K) at the zone bounded by the jet exit and

its development till jet impingement on the target plate for orifice diameters of 10 and 40 mm as an example for comparison . Both figures give the results for jet velocity of 18 m / sec and at axial positions of Xo =50 mm and 120 mm. Velocity distribution reveals air entrainment near the orifice exit and wall jet development on the target plate. Both figures indicate that smaller axial distances are with greater pressure created on the plate, big orifice diameter give higher static pressure values on the target plate and wider areas cover aged by the static pressure. Distribution of kinetic energy shows that the zones near the jet edges and that away from the stagnation zone on the target plate have the greatest kinetic energy within the flow ,this is clear for the d=40 mm results . The d= 10 mm results shows that the kinetic energy is noticed to have its maximum values near the stagnation zone for both axial positions tested . The mentioned results for both orifice sizes are in agreement with experimental results of reference (11), where high kinetic regions are noticed at the near wall region of the flat plate away from the stagnation zone.

The velocity distribution for the bigger orifice diameter indicates the convergence of orthogonal velocity to axial velocity direction starts within the area cove raged by the jet at the stagnation zone i-e within the orifice area for small axial distances or wider area for the bigger axial distances, this gives the chance to the existence of cross flow in this region .On the contrast such behavior is not noticed for small orifice diameters. The concentration of small diameter jets and high values of its pressure coefficients can be discussed on the mentioned wall jet flow at the stagnation point and it also give the reason for higher heat transfer rates noticed for small orifice diameters when compared to relatively bigger orifices as confirmed by the experimental results of reference (1) mentioned earlier . The existence of cross flow in the stagnation zone of big orifice diameter tends to reduce the heat transfer rates.

The experimental results for velocity distribution in the wall jet are shown in Figure (9) .The distribution for orifices diameters of d= 10,20,40 mm and jet velocity of 18 m / sec at two axial positions of the target plate show that the greater the distance from the plate will give lower velocities in the wall jet . The bigger the orifice diameter the lower percentage of impinging jet velocity converted to wall jet velocity components. Lower jet velocity of 7 m/ sec shows a wall jet percentages greater than that for higher jet velocities of 18 m/sec, this attributed to high rate of energy lost due to high turbulence levels conjugated with the higher jet velocities. Figure (10) represents the velocity distribution of the wall jet at different vertical positions from the target plate. The results give the same trend mentioned above with more gradual velocity distributions for the 40 mm orifice diameter than that for the 10 mm diameter. Figure (9) and Figure (10) results show that for d=10 mm the wall jet velocities is in the range of 10-80% of the jet velocity for Xo =50 mm while it is in the range of 10-60% for Xo= 120 mm. This percentage increases for d= 20 mm to range 20-98% and 20-85% for same mentioned axial distances respectively. Bigger orifice size of d=40 mm is noticed to have relatively lower percentages of wall jet velocities of 20-70% at Uj = 18 m/ sec At. Lower velocity of 7 m /sec , d=40 mm results give higher values of velocities' percentage which reaches about 95% of the impinging jet velocity.

The discussion of turbulence level in the shear layers of a planar given in reference (9) , indicates that the centre line zone or the core of the jet is characterized by low turbulence levels while the edge of the jet have the highest turbulence levels which is conjugated with maximum velocity gradients encountered in the flow .Velocity gradients in the jet after striking the plate within the stagnation zone is presented in Figure (11).The d=10 mm results indicates that velocity gradients for such small diameter have its maximum value near the stagnation zone at the point at which impinging jet starts to convert into a wall jet . The 40 mm results shows a fluctuating behavior at the area covered by the impinging zone of such orifice diameter, this condition implies that the small orifice diameters are with high levels of turbulence relative to the big orifice diameter which means an enhancement of heat transfer at stagnation zone of the small orifices . More detailed researches in this field are to be done in the future to confirm these notifications using sensitive hot wire anemometry.

CONCLUSIONS

The experimental and numerical CFD of the jet flow and its impingement on a target plate for variable orifice sizes of 10,20,30,40, mm shows the following notes

1- Velocity profile measurements of the impinging jet shows the existence of a potential flow at the orifice exit. At larger axial position wider bell shaped velocity profiles are noticed at which transition zone starts and then at further longer axial distances from the orifice the flow starts to convert to a zone at which the jet is known as a free jet.
2- A wall jet with a hydrodynamic velocity profile is formed on the target plate. Small orifice sizes are noticed to have greater velocity gradients near the stagnation zone compared to the big orifice size. Previous experimental investigations shows that the higher the velocity gradients , the higher is the turbulence generated at the stagnation zones which will lead to higher rates of heat removal at the stagnation zones of small orifice sizes.
3- Cross flow velocity vectors parallel to the plate wall are noticed in the flow field of the impinging jet of big orifice sizes. On the contrast such cross flow does not observed in the flow field of the small size orifices. Such trend of the existence of cross flow at the stagnation zone of the big orifice sizes and the region beyond it may be responsible for the experimentally noticed non linear increase of heat transfer with the increase of the orifice size. Reference (3) results confirm this observation.
4- The small orifice sizes are shown to have higher average pressure coefficients relative to the big orifice sizes due to concentrated static pressure on the target plate area and lower cross flow velocities with the higher jet velocity gives higher average pressure coefficient on the target plate. Calculated average pressure coefficients are in the range of 0.4-0.6.
5- The turbulent kinetic energy distribution results confirm the experimental results by references [7] and [11] which give the turbulence level and kinetic energy at the jet boundary edge and at the stagnation point and the zone beyond it and show that its values have the highest kinetic energy level in the flow.

6- Small orifice size tested of 10 mm are noticed to have higher velocity ratio of the wall jet velocity relative to the incoming or impinging jet velocity. The higher the jet velocity the greater is this ratio. On the contrast big orifices are shown to have lower velocity ratios, with the lower jet velocities of big size tested of 40 mm have higher velocity ratio of the wall.

REFERENCES

[1].Jung-Yang San, Chih- Hao Huang and Ming –Hong Shu, Impingement cooling of a confined circular air jet, Int. J. Heat Mass Transfer, **Vol** .40 no 6 pp. 1355-1364,(1997) .

[2].M. Behina, S. Parneix , Y.Shabany , P.A .Durbin, Numerical study of turbulent heat transfer in a confined and unconfined impinging jets , Into .J of heat and fluid flow , **Vol**.20 .pp 1-9 , (1999).

[3].R. J. Goldestien and A.I. Behbahani, Impingement of circular jet with and without cross flow, Int. J. Heat Mass Transfer, vol. 25, no .9, pp.1377-1382, (1982).

[4].D .Lee, R. Greif, S.J. Lee and J. H. Lee, Heat transfer from a flat plate to a fully developed ax symmetric impinging jet, Transactions of the ASME, **Vol**. 117, August, pp. 772-776, (1995) .

[5].A.K.Mohanty and A.A.Tawfek , Heat transfer due to round jet impinging normal to a flat surface , Int . J. Heat Mass Transfer, vol.36 no. 6 pp 1639-1643 , 1993) . .

[6].D. Lytle and B.W Webb, Air jet impingement heat transfer at low nozzle plate spacing, Int . J .Heat Mass Transfer **Vol**.37 no.12 pp .1687-1697,(1994) .

[7].J. Mi , G. J. Nothan , D. S. Nobers ,Mixing characteristics of ax symmetric free jets from a contoured nozzle ,an orifice plate and a pipe , Transactions of the ASME ,**Vol** 123 , December , pp.878-883 ,(2001) .

[8].E.Baydar , Y. Ozmen , An experimental and numerical investigation on a confined impinging air jet at high Reynolds numbers . Applied thermal engineering, Vol.25, issue 2-3, February, pp.409-421,(2005) .

[9].H.K.Versteg and W. Malalasekera, an Introduction to Computational Fluid Dynamics. The Finite Volume Method, Longman Scientific and Technical, United States, New York, (1995) .

[10].M.M. Hofmann , M. Kind , H. Martin , Measurements on steady heat transfer and flow structure and new correlations for heat band mass transfer to submerged impinging jet. Int .J. Heat Mass Transfer .**Vol** .50,pp 3957-3965 ,(2007).

[11].K.Nashino , M.Samada, K.Kasuya, and K. Torij ,Turbulence Statistics in the Stagnation Region Of an Ax symmetric impinging Jet Flow , Int J. Heat and Fluid Flow **Vol** . 17,pp 193-201 ,(1996) .

[12].M.D. Deshpande and R.N. Vaishnav, Submerged laminar jet impingement on a plane. *J. Fluid Mech.* **Vol**.**114**, pp. 213–236,(1982)

[13].S. Ashfort-Frost, K. Jambunathan and C.F. Whithney, Velocity and turbulence characteristics of a semi confined orthogonally impinging slot jet. *Exp. Thermal Fluid Sci.* **Vol**.**14**, pp. 60–67. (1997)

[14].A.M. Huber and R. Viskanta, Convective heat transfer to a confined impinging array of air jets with spent air exits. *ASME J. Heat Transfer* Vol. 116**,** pp. 570–576. (1994)

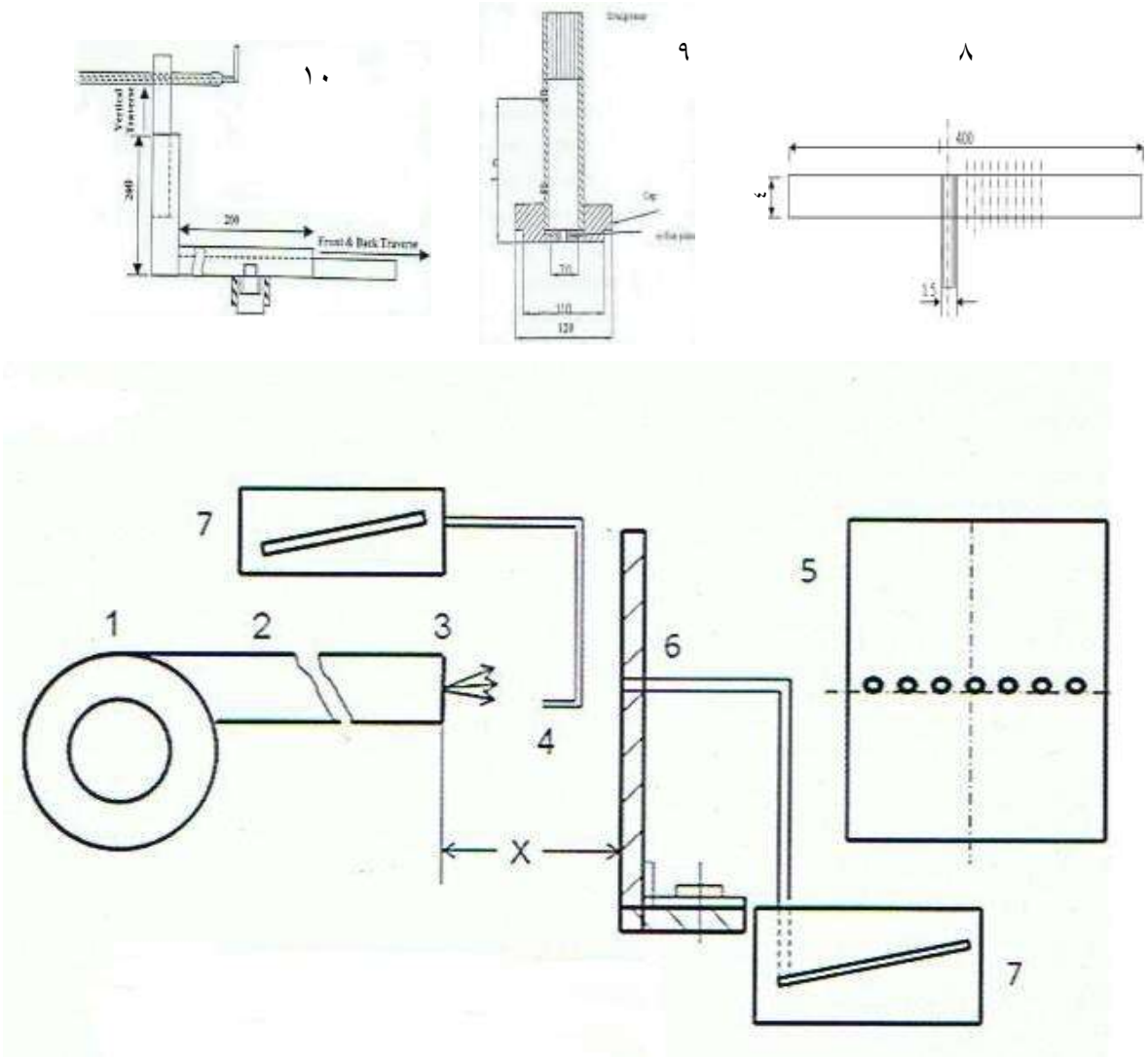

Figure(1) Test Rig Details ,1-blower 2-impingement pipe 3- orifice 4- total tube 5- target plate 6-static pressure tube 7- manometer 8- details of target plate 9- impingement pipe and orifice details 10- traversing mechanism.

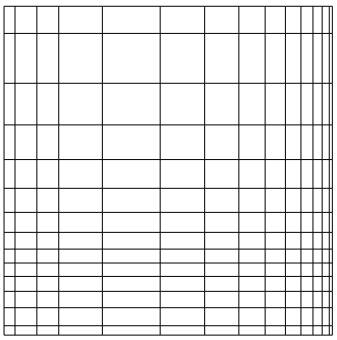

Figure (2) Mesh Used In CFD Calculations.

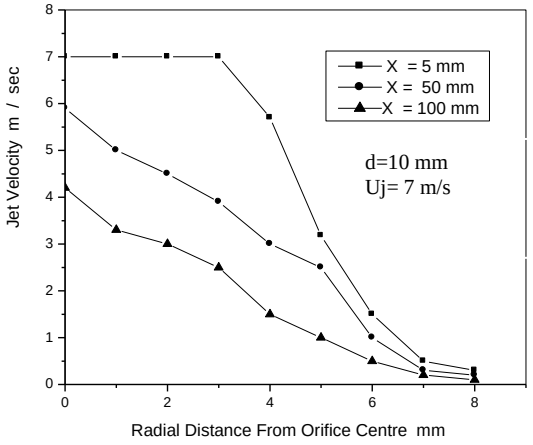

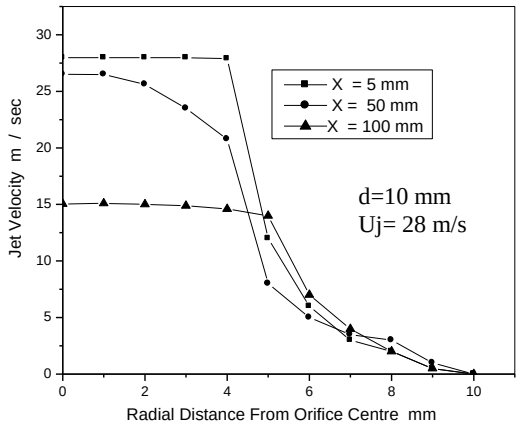

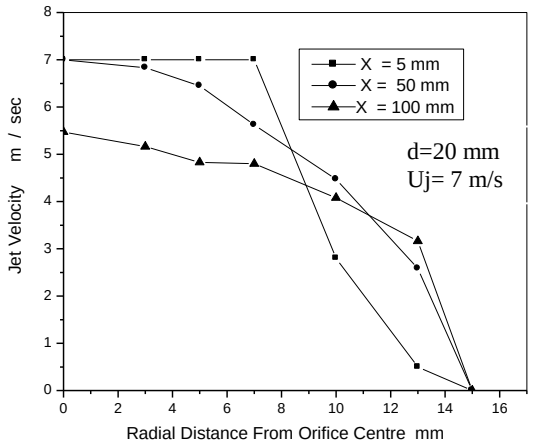

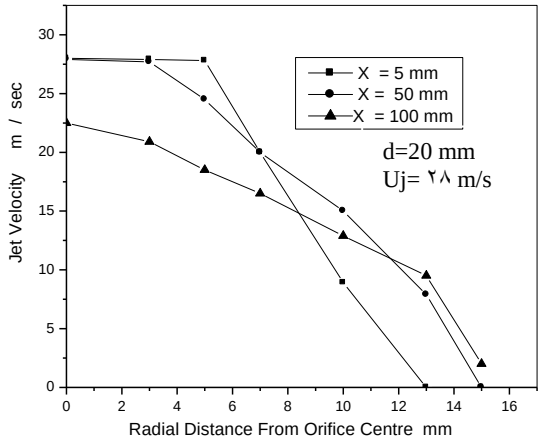

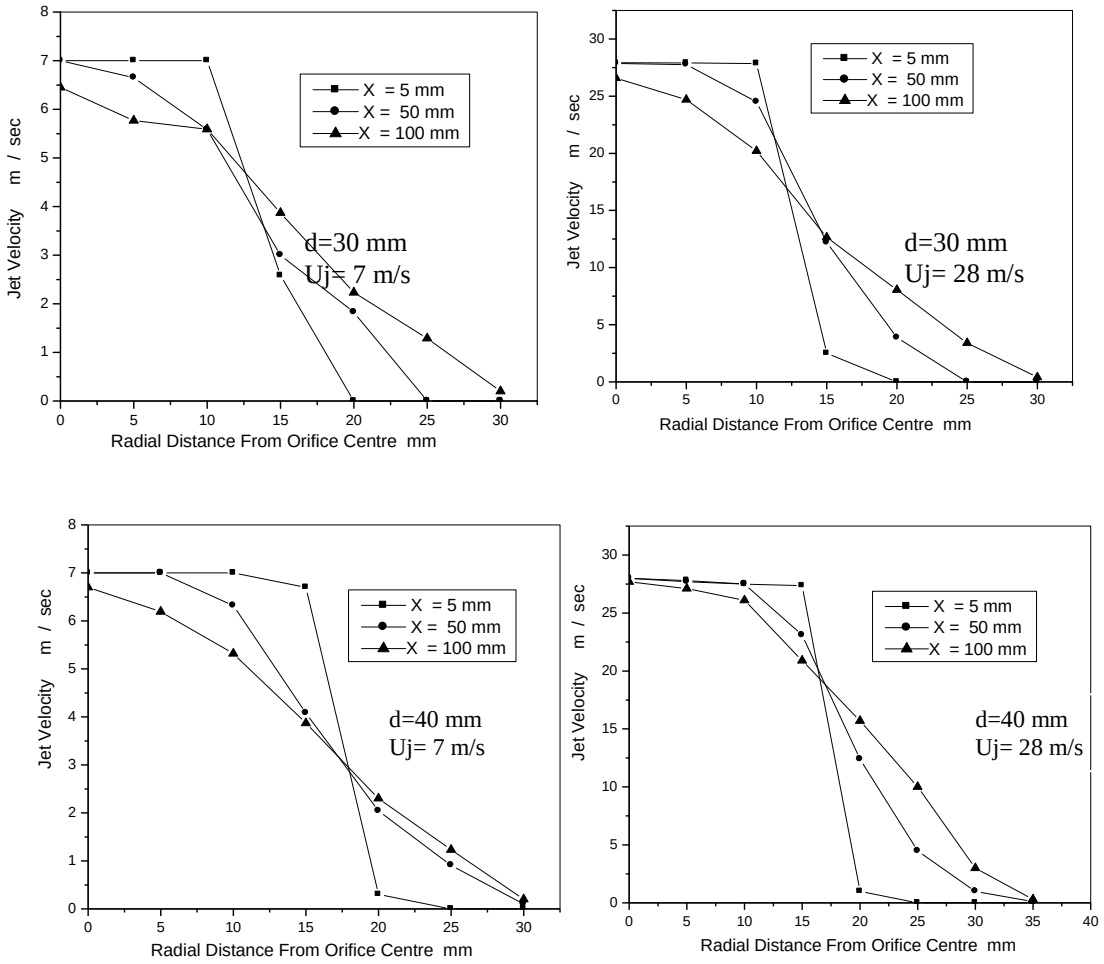

Figure (3) Jet Velocity Distribution At Orifice Exit for Different. Axial Distances

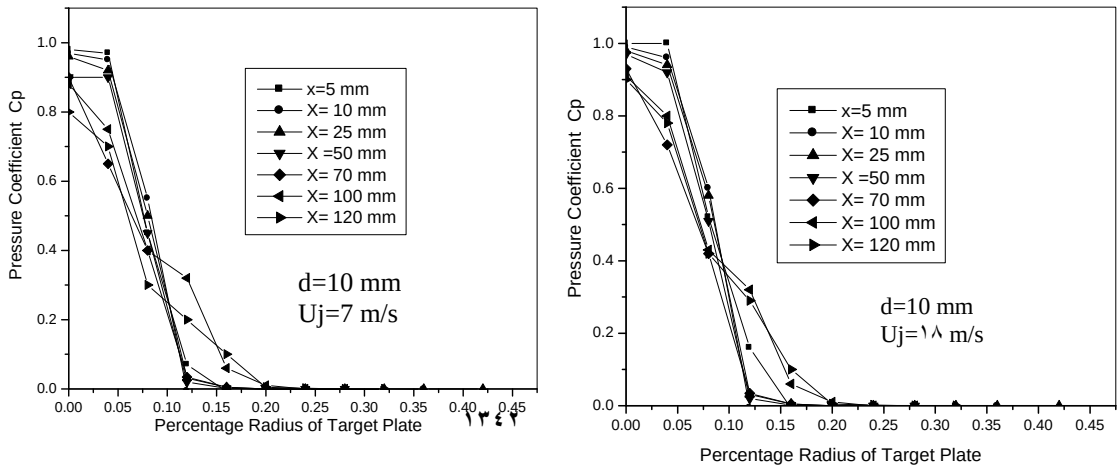

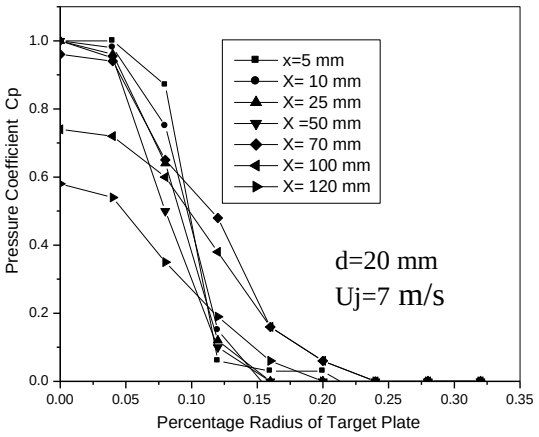
x=5 mm
X= 10 mm
X= 25 mm
X =50 mm
X= 70 mm
X= 100 mm
X= 120 mm
d=20 mm
Uj=7 m/s
Pressure Coefficient Cp
Percentage Radius of Target Plate

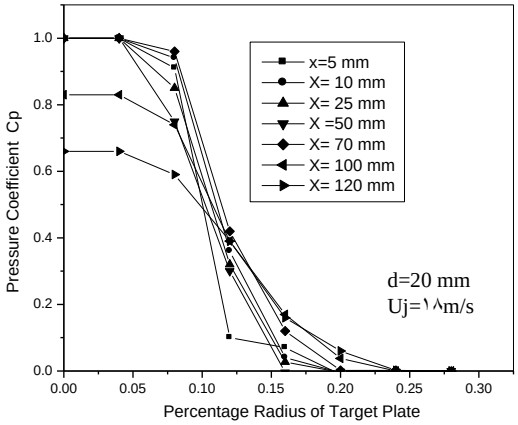
x=5 mm
X= 10 mm
X= 25 mm
X =50 mm
X= 70 mm
X= 100 mm
X= 120 mm
d=20 mm
Uj=١٨m/s
Pressure Coefficient Cp
Percentage Radius of Target Plate

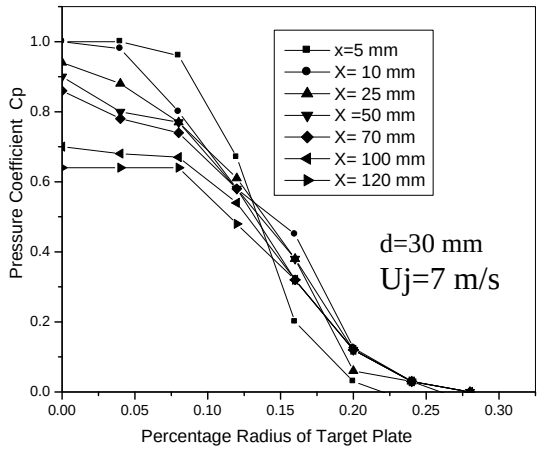
x=5 mm
X= 10 mm
X= 25 mm
X =50 mm
X= 70 mm
X= 100 mm
X= 120 mm
d=30 mm
Uj=7 m/s
Pressure Coefficient Cp
Percentage Radius of Target Plate

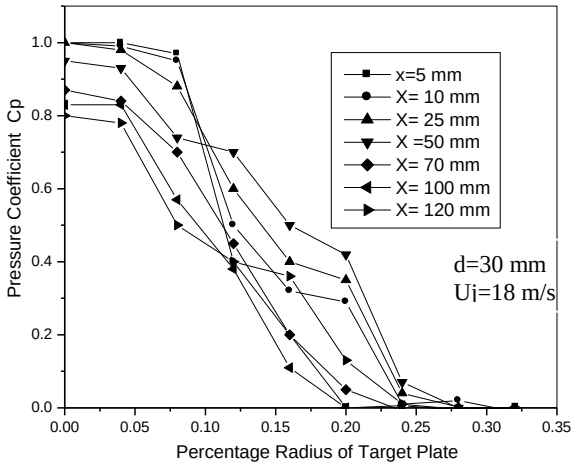
x=5 mm
X= 10 mm
X= 25 mm
X =50 mm
X= 70 mm
X= 100 mm
X= 120 mm
d=30 mm
Uj=18 m/s
Pressure Coefficient Cp
Percentage Radius of Target Plate

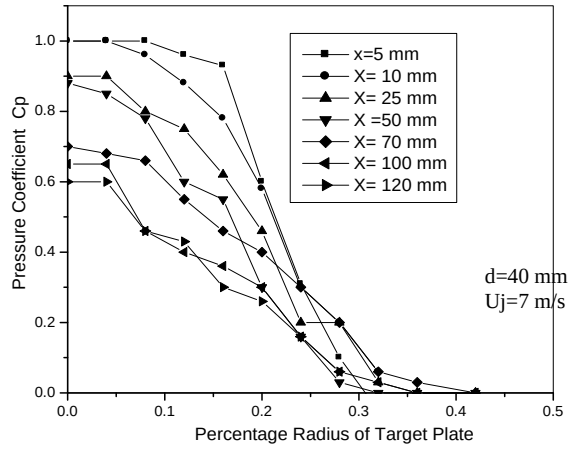
x=5 mm
X= 10 mm
X= 25 mm
X =50 mm
X= 70 mm
X= 100 mm
X= 120 mm
d=40 mm
Uj=7 m/s
Pressure Coefficient Cp
Percentage Radius of Target Plate

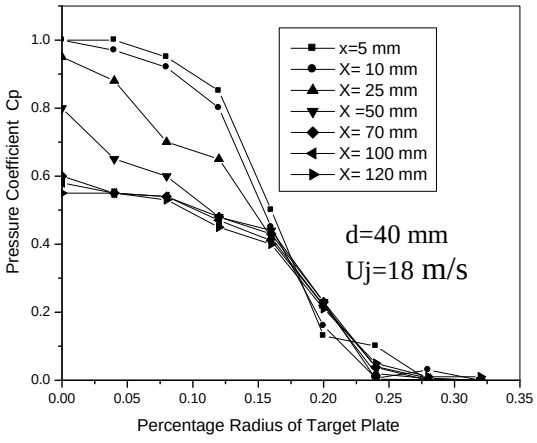
x=5 mm
X= 10 mm
X= 25 mm
X =50 mm
X= 70 mm
X= 100 mm
X= 120 mm
d=40 mm
Uj=18 m/s
Pressure Coefficient Cp
Percentage Radius of Target Plate

Figure (4) Pressure Coefficients At The Target Plate For Different Orifice Sizes. And Jet Velocities

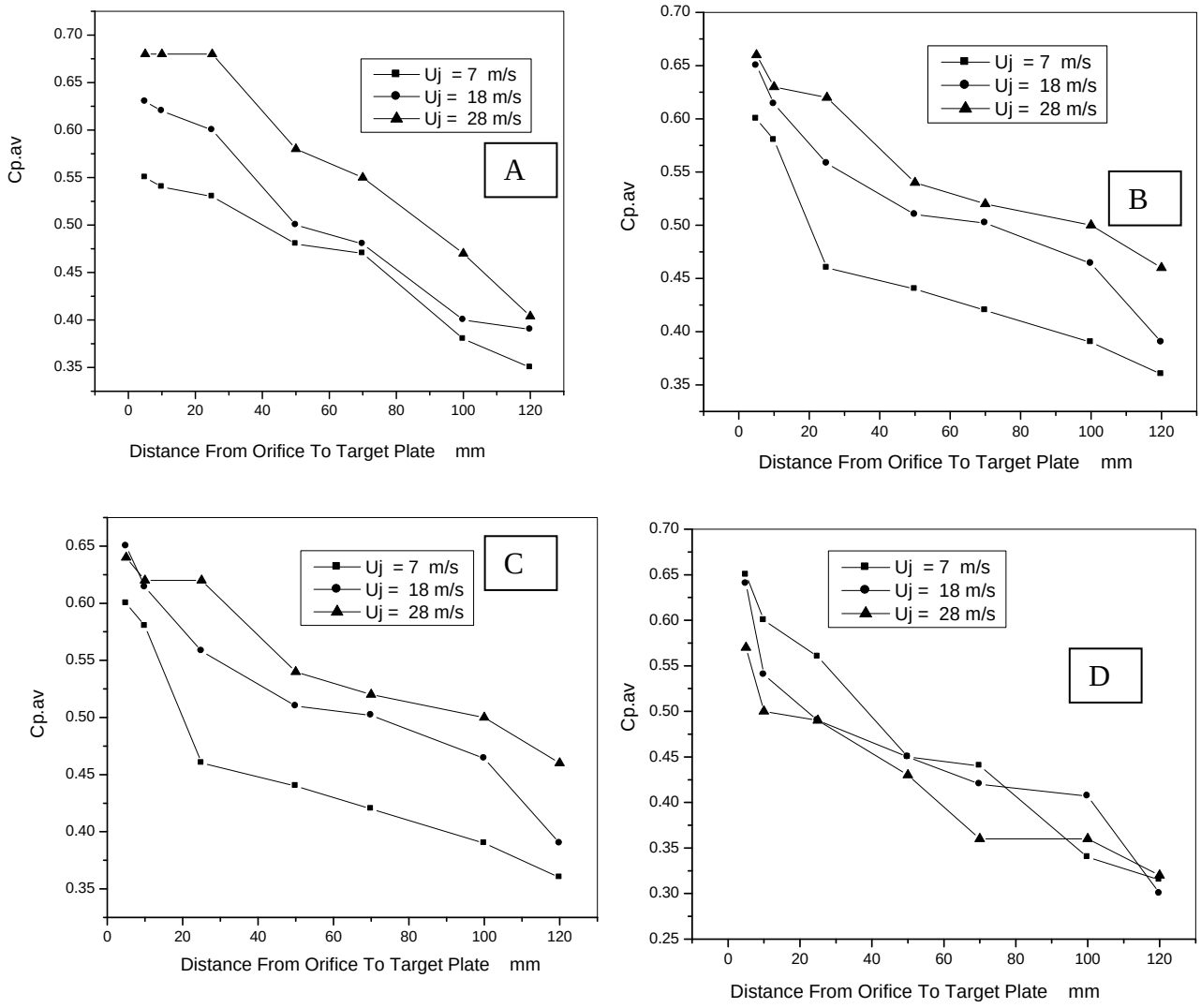

Figure (5)Variation Of Pressure Coefficient With Axial Distance From Orifice A-d= 10 mm , B- d= 20 mm , C- d= 30 mm , D- d= 40 mm

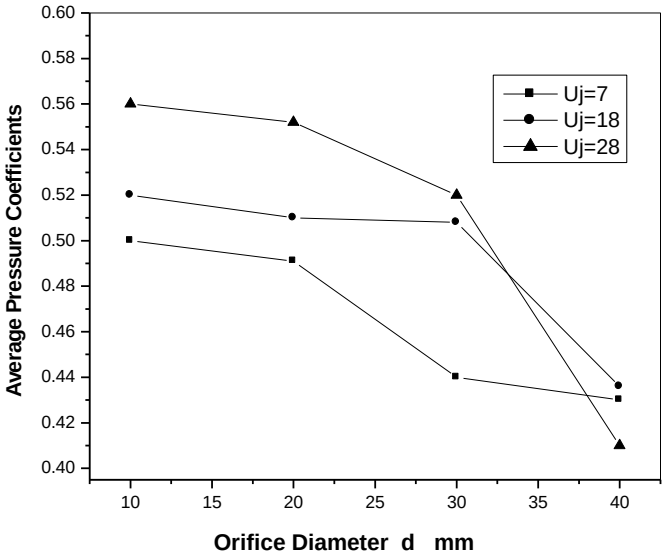

Figure (6) Average Pressure Coefficient On Target Plate With Orifice Diameter

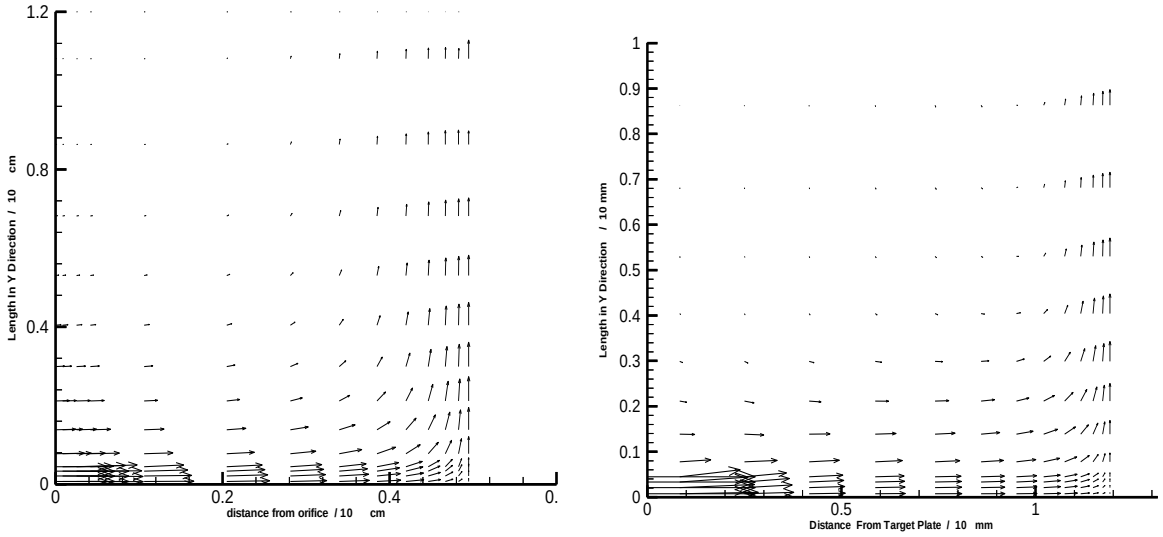

A

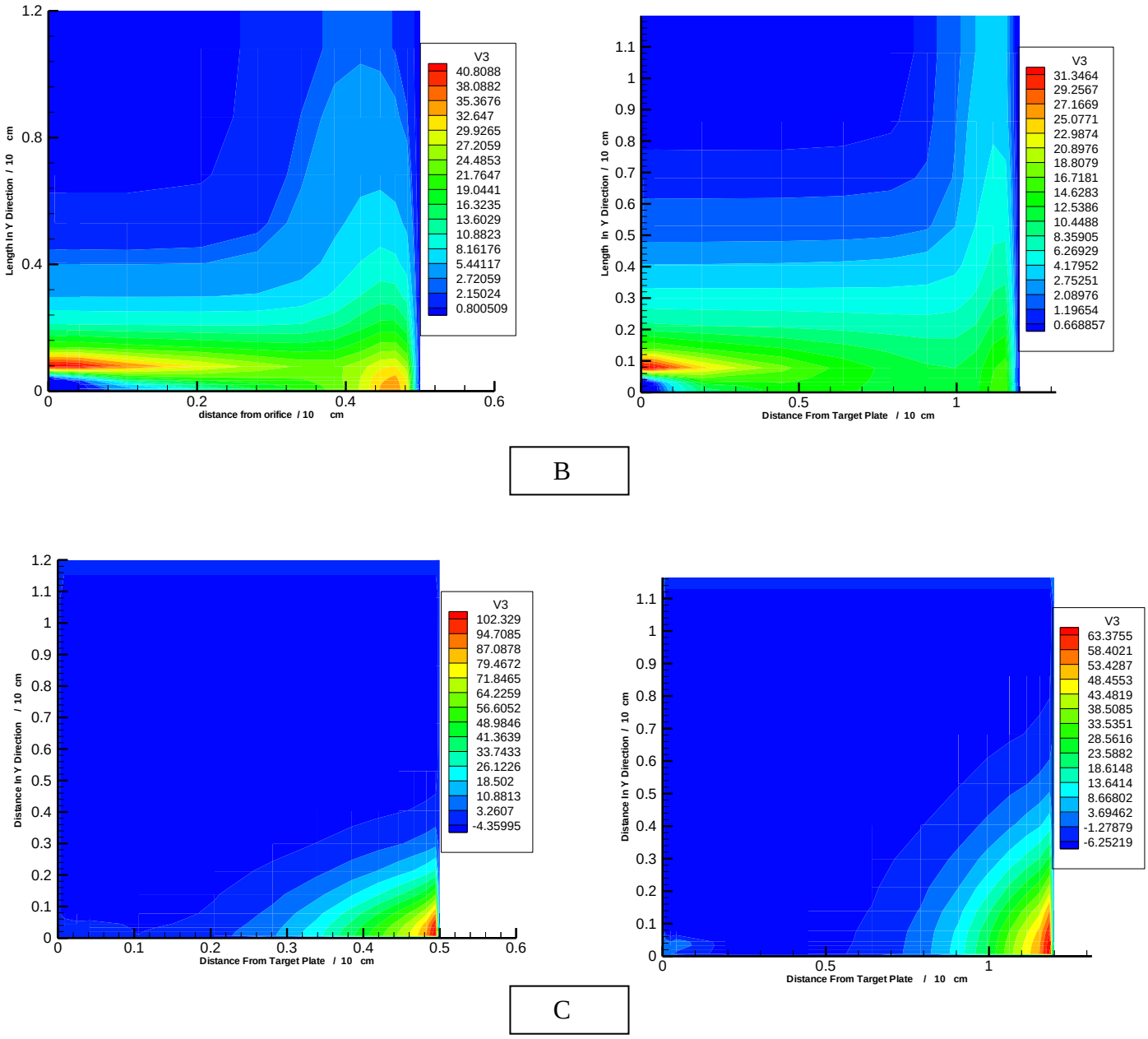

Figure (7) CFD Results For Orifice Diameter 10 mm ,Uj=18 m/sec A-velocity vectors (0.1 cm per m /sec) B-Turbulent Kinetic Energy K(m/sec)^2 C- Static Pressure N/ m^2

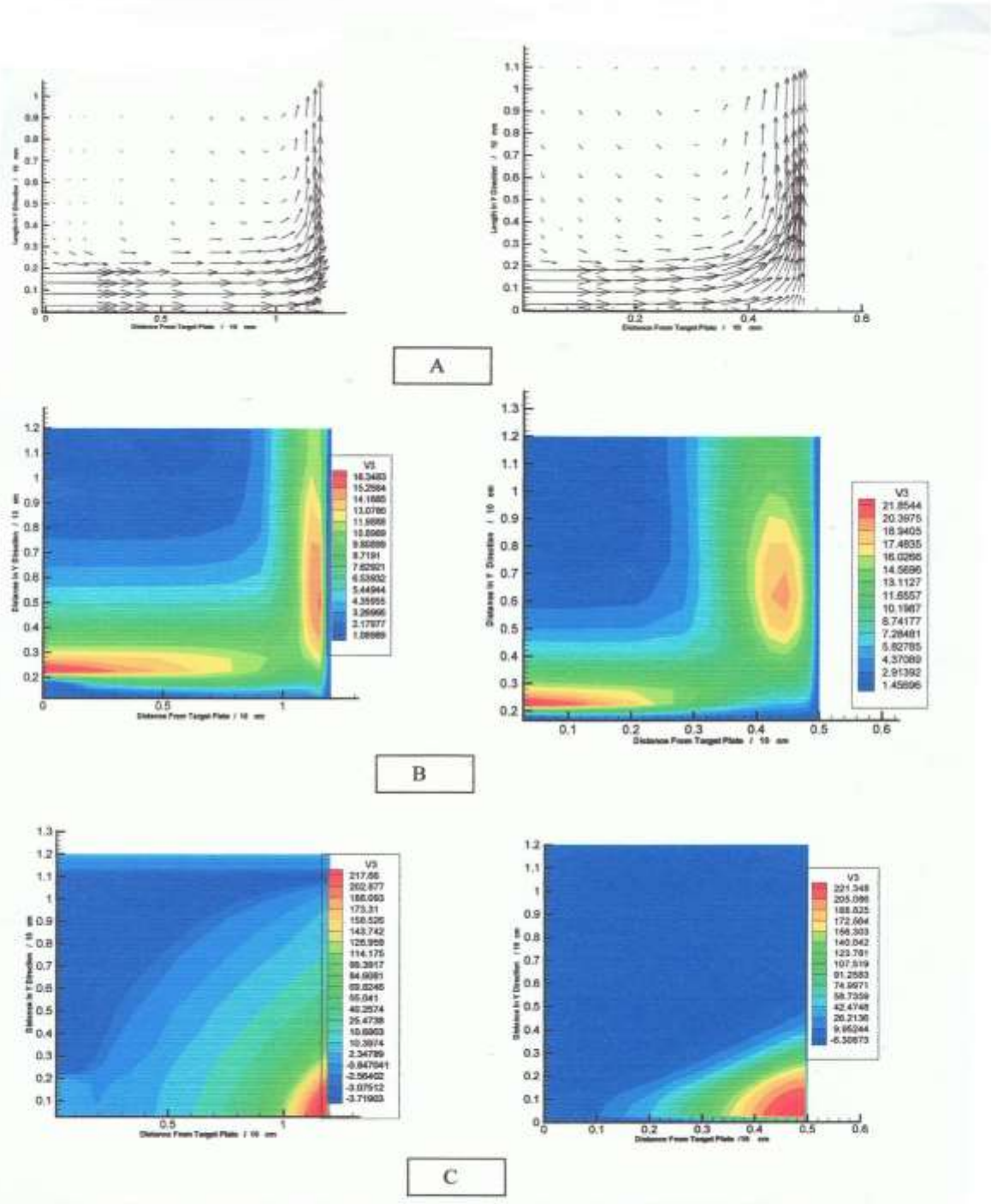

Figure (8) CFD Results For Orifice Diameter 40 mm, Uj=18m/sec A-velocity vectors (0.1)cm per m/sec) B-Turbulent Kinetic Energy K(m/sec)^2 C-Static Pressure N/m^2

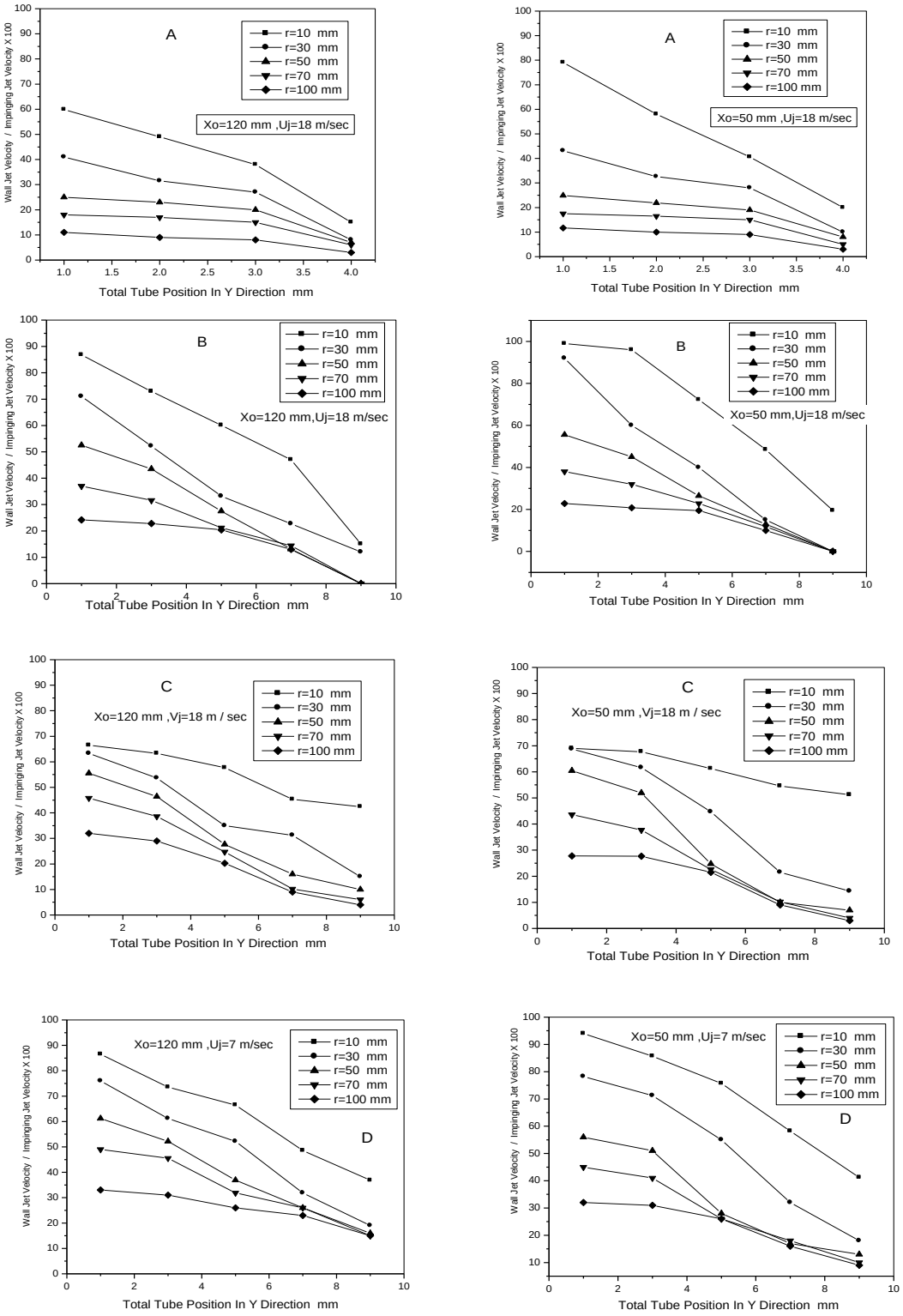

Figure (9)Velocity Distribution In The wall Jet For (A-d=10 mm, B-d=20 mm). & Uj=18 m/sec), (C -d = 40 mm ,Uj=18 m/sec) and (C -d = 40 mm ,Uj=7 m/sec)

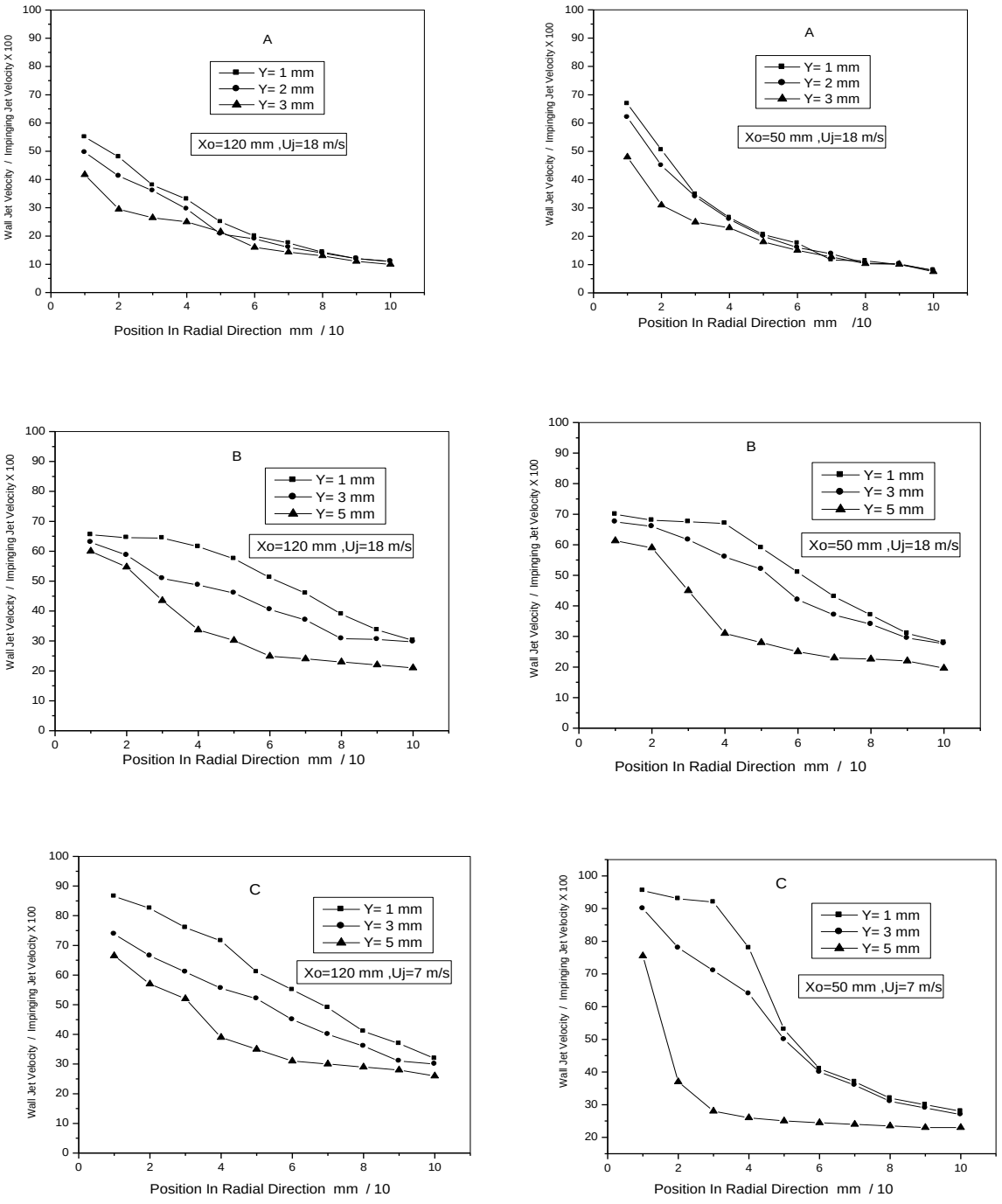

Figure (10) Velocity Distribution In the Wall Jet Region at Different Vertical Distances Y From the target Plate For A-(d=10 mm, Uj=18 m/sec), B-(d= 40 mm ,Uj= 18 m/sec) and C-(d=40 mm ,Uj = 7 m/sec).

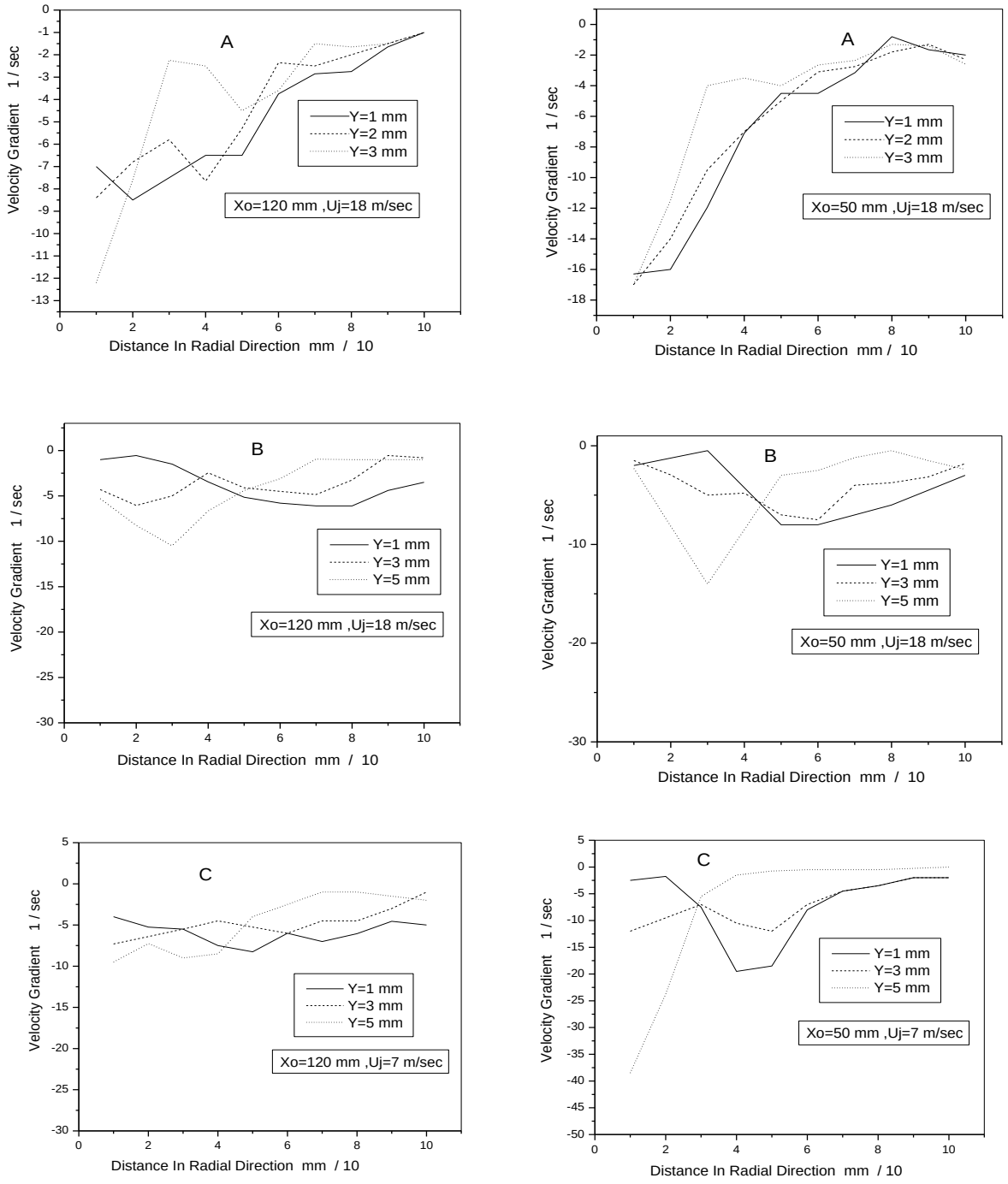

Figure (11) Velocity Gradients In the Wall Jet Region at Different Vertical Distances Y From the target Plate For A-(d=10 mm, Uj=18 m/sec), B- (d= 40 mm ,Uj= 18 m/sec) and C- (d=40 mm ,Uj = 7 m/sec).